J. Electrochem. Sci. Eng. **12(2)** (2022) 305-316; http://dx.doi.org/10.5599/jese.1191

Open Access : : ISSN 1847-9286

https://pub.iapchem.org/ojs/index.php/JESE

Original scientific paper

Modeling and synthesis of carbon-coated $LiMnPO_4$ cathode material: Experimental investigation and optimization using response surface methodology

Redouan El-Khalfaouy[1,2,✉], Khadija Khallouk[2], Alae Elabed[3], Abdellah Addaou[2], Ali Laajeb[2] and Ahmed Lahsini[2]

[1]*Laboratory of Natural Substances, Pharmacology, Environment, Modeling, Health and Quality of Life, Polydisciplinary Faculty of Taza, Sidi Mohamed Ben Abdellah University, B.P. 1223,Taza, Morocco*

[2]*Materials, Processes, Catalysis and Environment Laboratory, High School of Technology, Sidi Mohamed Ben Abdellah University, BP 2427, Fez, Morocco*

[3]*Microbial Biotechnology Laboratory, Faculty of Science and Technology, Sidi Mohammed Ben Abdellah University, BP. 2202, Fez, Morocco*

Corresponding author: ✉redouan.elkhalfaouy@usmba.ac.ma

Received: November 21, 2021; Accepted: January 17, 2022; Published: January 25, 2022

Abstract

Nanostructured $LiMnPO_4$ cathode materials for lithium-ion batteries (LIBs) have been successfully prepared by a modified solvothermal method under controlled conditions. Polyethylene glycol (PEG-10000) was used as a solvent to optimize the particle size/morphology and as a carbon conductive matrix. In order to investigate the effect of synthesis parameters such as concentration of PEG-10000, reaction time and reaction temperature on the $LiMnPO_4$ phase purity, Response surface methodology was carried out to find variations in purity results across the composition. The purity of all materials was checked using HighScore software by comparing the matched lines score to ones of reference data. As a result, it has been found that the pure phospho-olivine material $LiMnPO_4$ can be synthesized using the following optimum conditions: PEG concentration = 0.1 mol l^{-1}, reaction time = 180 min, and reaction temperature = 250 °C. The as-prepared $LiMnPO_4$ under optimum conditions delivered an initial discharge capacity of 128.8 mAh g^{-1} at 0.05 C-rate. The present work provides insights and suggestions for optimizing synthesis conditions of this material, which has been considered the next promising cathode candidate for high-energy lithium-ion batteries.

Keywords

Response surface methodology; olivine structure; solvothermal synthesis; PEG-10000; lithium-ion batteries

Introduction

Rechargeable lithium-ion batteries (LIBs) with high-energy, high power density, durability, and lightweight have become the most requested energy source in order to meet future society's needs in many renewable energy storage systems, starting from laptops, cell phones to electric vehicles. With the increasing demand for higher capacity and improved safety, many efforts have been made to further develop the next generation of LIBs with high volumetric/gravimetric energy density. Most commercial LIBs are currently based on $LiCoO_2$ layered structure as a cathode material. Therefore, one of the main challenges is to replace the commercialized layered structure cathode (which exhibits a theoretical specific capacity of 274 mAh g^{-1}) with other promising and efficient cathode materials.

$LiMPO_4$ (M = Fe, Mn, Co, Ni) olivine-based high-performance cathodes are the recommended alternative cathode materials to replace traditional ones ($LiCoO_2$) due to their low cost, non-toxicity, high thermal and cyclic stability, and environmental impact [1–5]. Compared to the first commercialized cathode, which is $LiFePO_4$, $LiMnPO_4$ is considered as the most promising cathode material in the next generation of lithium-ion batteries due to the high theoretical energy density (701 Wh/kg), which is higher than that of $LiFePO_4$ (586 Wh kg^{-1})[6,7]. Moreover, the low voltage (4.1 V *vs* Li/Li^+) of $LiMnPO_4$, which is positioned within the stable window of the most commercialized electrolytes, makes it the best candidate material compared to $LiCoPO_4$ and $LiNiPO_4$, which have higher potentials, being respectively 4.8 and 5.1 V *vs.* Li/Li^+ [8–10].

However, $LiMnPO_4$ exhibits significantly lower electrochemical performances than $LiFePO_4$ because of two important drawbacks that limit its electrochemical activity, including low electronic conductivity (<10^{-10} S/cm) being even lower than that of LFP (10^{-9} S cm^{-1}), and low lithium-ion diffusion rate ≈10^{-16} cm^2 s^{-1} [11,12]. Furthermore, the anisotropic distortion of the Jahn-Teller lattice in the Mn^{3+} sites and the interface strain during phase transitions between the lithiated and delithiated phases ($LiMnPO_4$-$MnPO_4$) cause a significant volume change (≈8.9 %) compared to $LiFePO_4$-$FePO_4$ (≈7 %) [13,14]. Recently, many attempts have been reported to overcome these limitations [15–17]. The results confirmed that particle size reduction could strongly increase the lithium-ion diffusion during the charge/discharge process [17–19]. The same behavior has been reported by the surface carbon coating [20–22], and the partial substitution of transition elements [23–26].

The synthesis process was also considered a direct approach to achieving desired performances. For this reason, several methods have been applied to prepare $LiMnPO_4$ with high purity, such as spray-pyrolysis [22,27], sol-gel method [28,29], hydrothermal synthesis [30–33], precipitation method [34,35] and solution combustion process [36,37]. Among all these methods, some selected ones offer more advantages such as morphology control, better homogeneity, submicron-sized particles, and larger specific surface area with increased electrochemical performances [38,39]. The solvothermal technique has significant assets compared to other methods such as simplicity to handle, short reaction time, moderate reaction temperature, good crystallinity and high purity [40,41]. The process is widely used for preparing various micro and nanostructured materials such as cathodes/anodes, oxides, semiconductors, ceramics, *etc.*

However, morphology and particle size are difficult to control since they are determined by many factors such as precursor types, additives or surfactants, pH, reaction time/temperature, and physico-chemical properties of the used solvent. Polyethylene glycol (PEG) is an organic solvent that can be easily adsorbed on the crystal's surface by hydrogen bonding, consequently influencing nucleation and crystallite growth.

Based on these advantages of PEG, we report in this work the synthesis of $LiMnPO_4$ cathode material under solvothermal conditions, using the PEG-10000 as a solvent to optimize particle size/morphology and as a carbon-coated source. To the best of our knowledge and after a thorough literature review, no study is presented on optimizing the synthesis parameters of $LiMnPO_4$ using the Response Surface Method (RSM). Figure 1 is a schematic representation of $LiMnPO_4$ synthesis and analysis performed in this work.

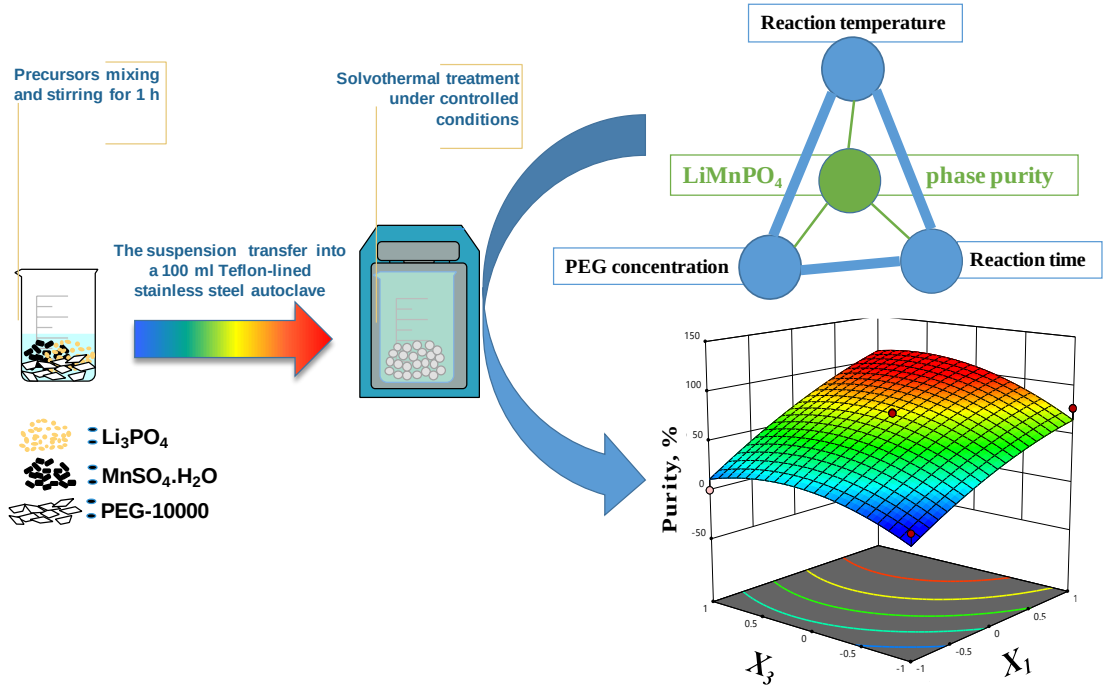

***Figure 1**. Schematic figure for $LiMnPO_4$ synthesis and analysis*

Experimental

Materials preparation

All chemical precursors are of analytical grade and used without any further purification. The cathode $LiMnPO_4$ was prepared *via* facile solvothermal reaction using the following raw precursors; Li_3PO_4, $MnSO_4.H_2O$ (99 %, Sigma Aldrich) and PEG-10000 (flakes, Sigma Aldrich). Firstly, Li_3PO_4 intermediate compound was prepared by mixing Li_2CO_3 (99 %, Honeywell Fluka) with $(NH_4)_2HPO_4$ (99 %, Merck) and citric acid (2M) (99.5 %, Merck) in appropriate amounts under magnetic stirring and heat at 90 °C for 60 min. The resulted product was filtered, washed with deionized water (DW) and dried overnight. Then, $MnSO_4{\cdot}H_2O$, Li_3PO_4, and PEG-10000 (with different concentrations: 0.00, 0.05 and 0.1 M) solvent were mixed under vigorous stirring for 60 min. The suspension was transferred into a 100 ml stainless steel autoclave followed by thermal treatment at different temperatures, *i.e.,* 150, 200 and 250 °C for a certain reaction time ranging from 60 to 180 min. The autoclave was then taken out of the furnace and cooled down to room temperature. The obtained products were washed with distilled water several times, collected by filtration, and finally dried at 80 °C overnight. Surface carbon coating of $LiMnPO_4$@C was activated by sintering the as-prepared products at 700 °C for 6 hours under argon atmosphere with a heating rate of 5 °C min^{-1}.

Experimental design and statistical analysis

The Box-Behnken design was used for the response methodology to examine the relationship between one or more dependent response variables and a set of quantitative experimental factors

(independent variables). A mathematical model, followed by the second polynomial equation, was developed to describe the relationship between the predicted response variable (matching lines score (purity) of the synthesized $LiMnPO_4$) and the independent variables of solvothermal synthesis conditions. It was described by eq. (1)

$$Y_{LiMnPO_4} = \beta_0 + \sum_{i=1}^{3} \beta_i X_i + \sum_{i=1}^{3} \beta_{ii} X_i^2 + \sum_{i=1}^{3} \sum_{i \neq j=1}^{3} \beta_{ij} X_i X_j \quad (1)$$

where Y_{LiMnPO_4} is the predicted response variable, X_i, X_j ($1 \leq i, j \leq 3$; $i \neq j$) represent the coded independent variables (solvothermal conditions), β_0 is the intercept coefficient, β_i are linear terms, β_{ii} are squared terms, and β_{ij} are interaction terms.

This study used this design to determine the effect of three factors (PEG concentration, solvothermal reaction time and temperature) on $LiMnPO_4$ phase purity. The ranges and levels of the experimental parameters are depicted in Table 1. The Design-Expert12 software was used to analyze the results of all experiments.

Table 1. *Experimental ranges and levels of independent variables*

Variables	Symbol	Level		
		-1	0	1
PEG concentration, mol l^{-1}	X_1	0	0.05	0.1
Reaction temperature, °C	X_2	150	200	250
Reaction time, min	X_3	60	120	180

Structural, morphological and electrochemical characterization

Crystalline structure and phase purity of all products were analyzed and evaluated by X-ray diffraction using diffractometer PANalytical's X'Pert PRO, with Cu Kα radiation (λ = 1.5418 Å). The surface morphology and the chemical compositions were observed with a scanning electron microscope (FEI QUANTA 200) equipped with EDS for microanalysis of the surface.

The electrochemical tests were performed at room temperature in the potential range between 2.5 and 4.5 V using battery test systems (BaSyTec GmbH, Germany). All experiments were conducted using coin-type cells (CR2032) assembled according to our previous work [25].

Phase and morphology of the intermediate compound Li_3PO_4

All detectable peaks of the as prepared Li_3PO_4 are shown in Figure 2, where the peaks are indexed as Li_3PO_4 according to the standard data PDF # 071-1528.

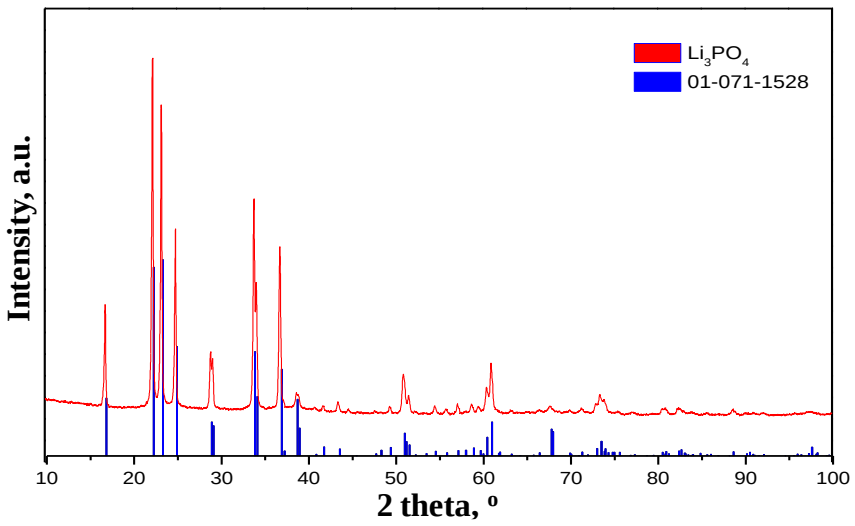

Figure 2*. XRD patterns of as-prepared Li_3PO_4 intermediate compound*

Based on the matching lines score, no impurity-related peaks could be detected, indicating a high level of purity of the as-prepared Li_3PO_4 material. The prepared sample has an orthorhombic crystal structure with a $Pmn2_1$ space group.

Figure 3 shows SEM images of the Li_3PO_4 product at different magnifications, which suggest that the product is of an irregular nanoplate-like structure. The present results are in good agreement with the literature [33,42]. The microstructure of Li_3PO_4 was studied by energy dispersive spectroscopy (EDS) to obtain the elemental composition. The collected EDS results shown in Figure 3, confirm the presence of only P and O atoms with a high amount of carbon (from the sample holder and citric acid), without the appearance of any other element.

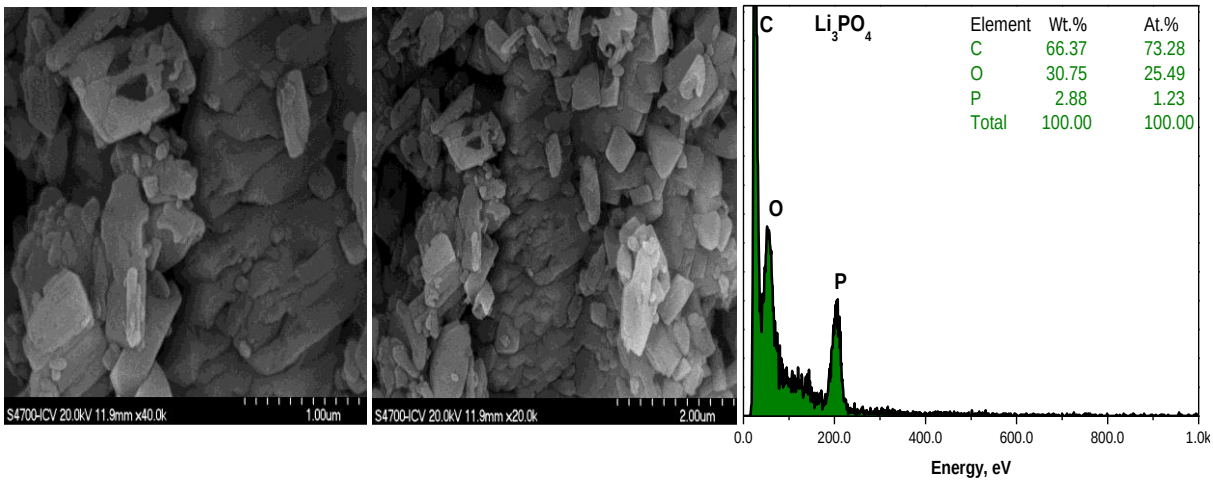

Figure 3. *SEM images and EDS spectrum of the as-prepared Li_3PO_4*

Results and discussion

Effect of operating conditions on $LiMnPO_4$ phase purity

The design matrix composed of 17 experiences, along with their experimental and predicted responses, are shown in Table 2.

Table 2*. Experimental design matrix proposed for $LiMnPO_4$ phase purity*

Run	X_1	X_2	X_3	Matching lines score with reference data #01-074-0375, %	
				Experimental	Predicted
1	0	0	0	75.00	74.60
2	0	0	0	73.00	74.60
3	-1	1	0	12.00	5.75
4	0	0	0	75.00	74.60
5	-1	0	1	10.00	11.75
6	1	1	0	99.00	93.25
7	1	-1	0	91.00	97.25
8	0	0	0	74.00	74.60
9	0	0	0	76.00	74.60
10	0	1	1	50.00	44.50
11	1	0	-1	77.00	65.25
12	0	1	-1	30.00	32.50
13	0	-1	-1	11.00	16.50
14	-1	-1	0	6.00	11.75
15	1	0	1	100.00	99.25
16	-1	0	-1	3.00	8.25
17	0	-1	1	88.00	70.50

The results show good agreement between experimental and predicted responses. The matched lines score with reference data#01-074-0375 (purity) of $LiMnPO_4$ was found to range from 3 to 100 %.

Based on the results presented in Table 2, the coefficients of the developed model in eq. (1) are estimated using multiple regression analysis technique. The polynomial model for the phase purity of $LiMnPO_4$ is represented by eq. (2):

$$Y_{LiMnPO_4} = 74.60 + 43.25X_1 - 2.50\,X_2 + 16.50X_3 + 0.50X_1X_2 + 6.50X_1X_3 - \\ - 10.50X_2X_3 - 9.30X_1^2 - 13.30X_2^2 - 20.30X_3^2 \quad (2)$$

The fit quality of the $LiMnPO_4$ purity model was attested with an analysis of variance (ANOVA) [43]. Generally, the suitability of the model is confirmed by higher Fisher's value (*F*-value) with probability (*p*-value) as low as possible ($p<0.05$)[44]. Table 3 shows the analysis of variance (*F*-test) and the p-value for this experiment. The *p*-value of this model is about 0.0002, which indicates that the model was suitable for use in this experiment.

Table 3. *Analysis of variance (ANOVA) for the fitted quadric polynomial model for optimization of $LiMnPO_4$ phase purity*

Source	Degree of freedom	Sum of squares	Mean square	*F*-value	*p*-value
Model	3	17192.50	5730.83	14.61	0.0002
Residual	4	5.20	1.30	-	-
Corrected total sum of squares	17	72621.00	4271.82	-	-
$R^2 = 0.93$					
Adjusted $R^2 = 0.90$					

The calculated *F*-value for the regression is higher than 14, much higher than the value from Fisher tables ($F_{3,4} = 6.69$, for a 95 % confidence level), confirming that the model is well fitted to the experimental data [45,46]**.**

The determination coefficient (R^2) quantitatively evaluates the correlation between the experimental data and the predicted responses [47]. With $R^2 = 0.93$, we conclude that the predicted values match the experimental values perfectly. The adjusted $R^2 \approx 0.90$ is very close to the corresponding R^2 value, which confirms that the model is highly significant [48].

The regression coefficients of eq. (2) and the corresponding p-values are presented in Table 4. From this result, we can conclude that the linear effect of PEG concentration (X_1) and reaction time (X_3) are the principal determining factors for the response on $LiMnPO_4$ phase purity.

Table 4. *Estimated regression coefficients and corresponding p-values obtained during Box-Behnken design for $LiMnPO_4$ material purity:*

Parameter	Term	Estimate regression coefficient	Standard error	*F*-value	*p*-value
β_0	Intercept	74.60	6.26	12.05	0.0017
β_1	X_1	43.25	4.91	77.50	< 0.0001
β_2	X_2	-2.50	4.91	0.2589	0.6265
β_3	X_3	16.50	4.91	11.28	0.0121
β_{11}	X_1X_1	-9.30	6.77	1.89	0.2120
β_{12}	X_1X_2	0.5000	6.95	0.0052	0.9446
β_{22}	X_2X_2	-13.30	6.77	3.86	0.0903
β_{13}	X_1X_3	-10.50	6.95	2.28	0.1745
β_{23}	X_2X_3	6.50	6.95	0.8752	0.3807
β_{33}	X_3X_3	-20.30	6.77	8.99	0.0200

The response surface plot as a function of PEG concentration (X_1) and reaction time (X_3) is presented in Figure 4(a). X_1X_3 was chosen as the interaction key, which exhibits a low p = 0.1745 compared to others that are not significant (since they exhibit a p-value higher than 0.1) [49,50].

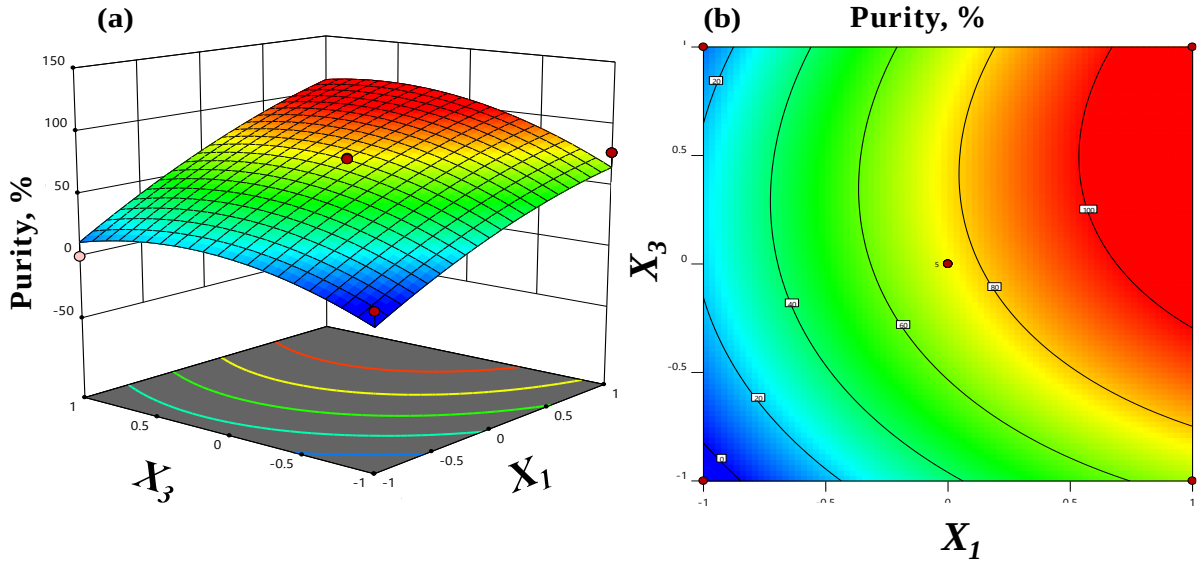

***Figure 4**. 3D response surface (a) and contour plot (b) of $LiMnPO_4$ phase purity for different coded values of X_1 (PEG concentration) and X_3 (reaction time)*

The combined effects of the two factors are positive and statistically significant, as also revealed by the contour lines presented in Figure 4(b). The optimum conditions for maximum $LiMnPO_4$ phase purity are as follows: c_{PEG} = 0.1 mol l^{-1}, T = 250 °C and τ = 180 min.

The synthesized material $LiMnPO_4$ under optimum conditions was characterized by X-Ray diffraction to confirm the phase purity. Figure 5 shows XRD results of the pure sample before and after calcination. It is clearly seen that the two patterns are very similar, with a difference in the peaks intensity which is much higher for the calcined sample. It is also observed that thermal treatment has not a remarkable effect on the formation process of the $LiMnPO_4$ phase and does not change the purity of the material, which indicates that the reaction has been done in the autoclave under solvothermal/optimum conditions. On the other hand, the main objective of calcination is the conversion of PEG layer adhered on the surface of the particles to the carbon layer, which promotes a higher electronic conductivity and consequently an improvement of the electrochemical performances.

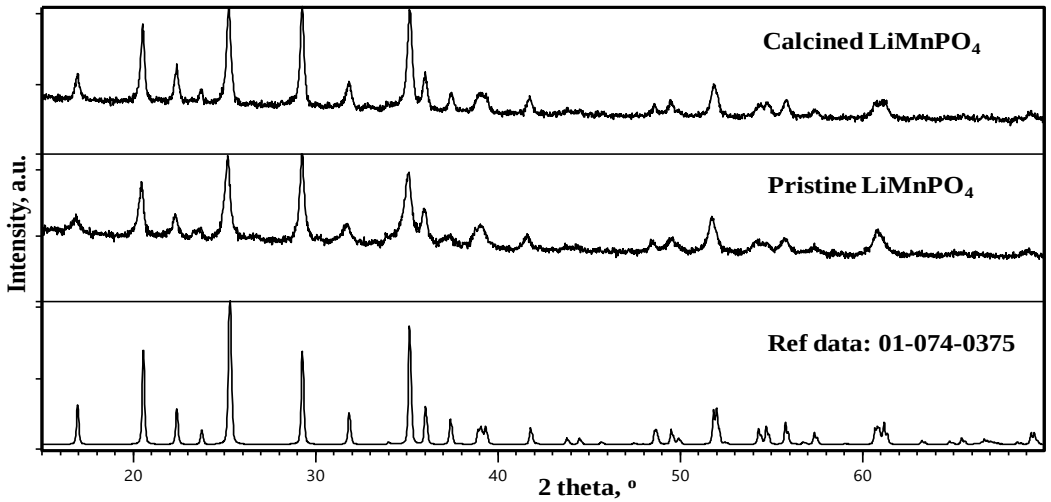

***Figure 5.** XRD patterns of pristine and calcined $LiMnPO_4$ material synthesized under optimum conditions*

The obtained results also confirm that a pure phospho-olivine structure $LiMnPO_4$ can be generated with a PEG-10000 concentration of 0.1 mol l^{-1}, a reaction temperature of 250 °C and a reaction time of 180 min. This pure phase was indexed as $LiMnPO_4$ crystal structure according to the standard data #01-074-0375, crystallizes in the orthorhombic system with the Pmnb space group.

During the thermal treatment process, most materials are generally subjected to some changes in the crystal structure, *i.e.*, crystallite size and microstrain (such as crystal lattice defects, stacking errors, displacement, *etc.* [51]). In order to verify these two parameters, both samples before and after calcination were examined by the Williamson - Hall (W-H) method as explained previously [35,36]. The W-H curves for all samples are displayed in Figure 6.

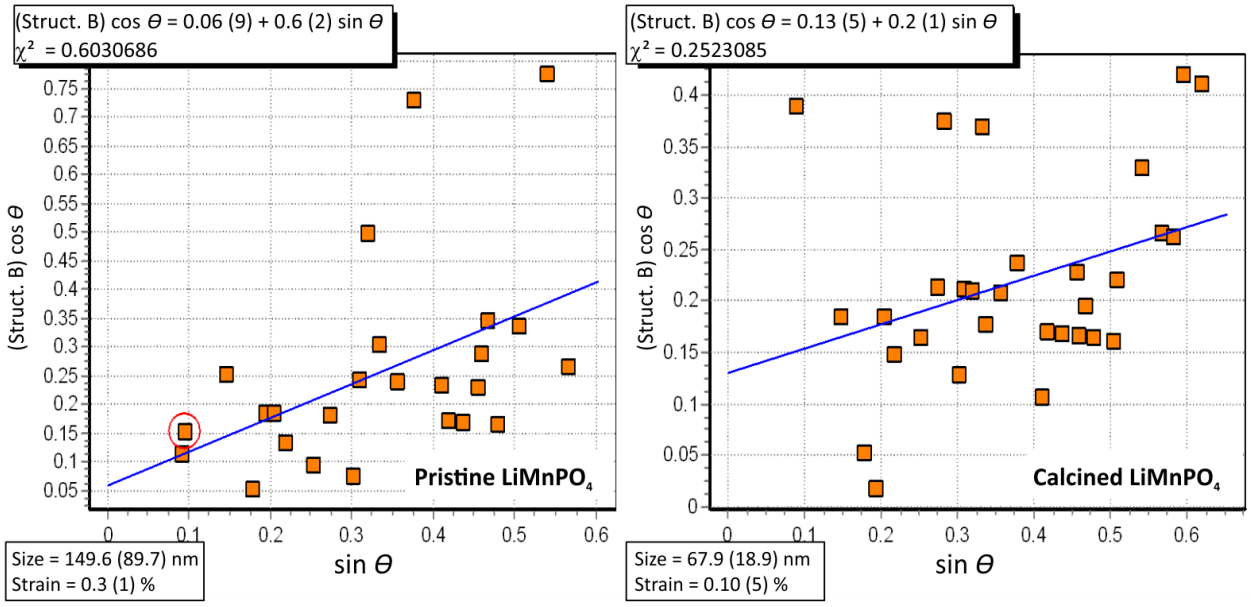

Figure 6. *Williamson-Hall plots of pristine and calcined $LiMnPO_4$ obtained under optimum conditions (Struct.B means structural broadening)*

According to these results, we can state that the crystallites size after calcination is about 68 ± 19 nm, which is strictly lower than that of the pristine material (150 ± 90 nm). This difference could be due to the thermal process that leads to the coalescence of the polyethylene glycol particles remaining adhered to the $LiMnPO_4$ material surface during the synthesis steps, leading to the formation of smaller, well-carbonated nanocrystallites. The lowest microstrain value of about 0.1 ± 5 % was observed for the calcined sample, while the highest strain value of 0.3 ± 1 % was detected for the pristine one. It can be noticed that crystal lattice defects can be reduced using an optimized PEG-10000 concentration, which can act as a protective matrix during the synthesis process due to the viscous property of this solvent.

Figure 7 shows the corresponding SEM images of the obtained products, pristine $LiMnPO_4$ and calcined $LiMnPO_4$@C materials. The surface morphology of the pristine sample seems like particles embedded in a polyethylene glycol matrix. However, the calcined sample image shows irregular secondary particles, with degradation of PEG matrix formed during synthesis steps, which confirms the transformation of PEG particles still adhered on the $LiMnPO_4$ material surface to a thin carbon layer.

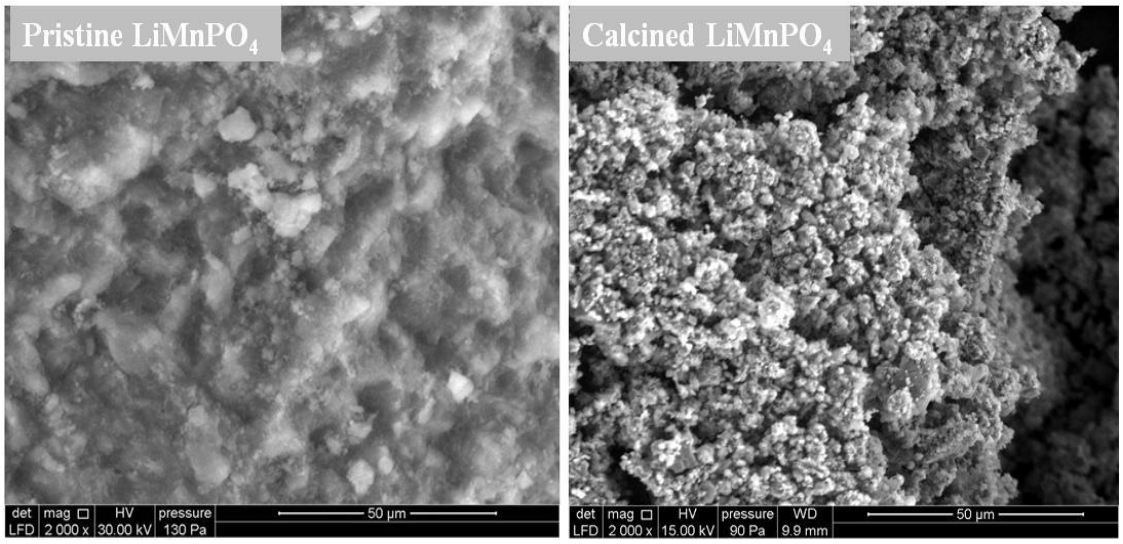

Figure 7. *SEM images of the synthesized pristine and calcined $LiMnPO_4$ material under optimum conditions*

Electrochemical performance of calcined $LiMnPO_4$@Ccathode material

The charge-discharge behavior of the calcined $LiMnPO_4$@C obtained under optimum conditions was studied using the "galvanostatic charging–discharging" method in the potential range of 2.5 to 4.5 V. As seen in Figure 8, the charge-discharge curves of the 1st, 2nd and 3rd cycles exhibit clear charge/discharge plateaus around 4.25 and 4.05 V, which is in agreement with the electrochemical de-lithiation/lithiation process, respectively [52]. The initial charge-discharge specific capacities were 164.8 and 128.8 mAh g^{-1} at 0.05 C-rate, respectively, which can be mainly attributed to the nanostructured crystallite size with the reduced microstrain that promotes good inter-calation/disintercalation of lithium ions within $LiMnPO_4$@C material structure [36,53]. Our findings are in good agreement with some previous works, where it was confirmed that $LiMnPO_4$ olivine structure without impurity could generate improved electrochemical performances [54]. However, the initial coulombic efficiency of about 78.2 % is mainly affected by unavoidable passivation phenomena of the electrolyte and the active electrode materials [55].

The as-prepared material under optimum synthesis conditions will be subjected to a wide range of electrochemical characterization in order to fully explain the different reaction mechanisms during the charge-discharge process.

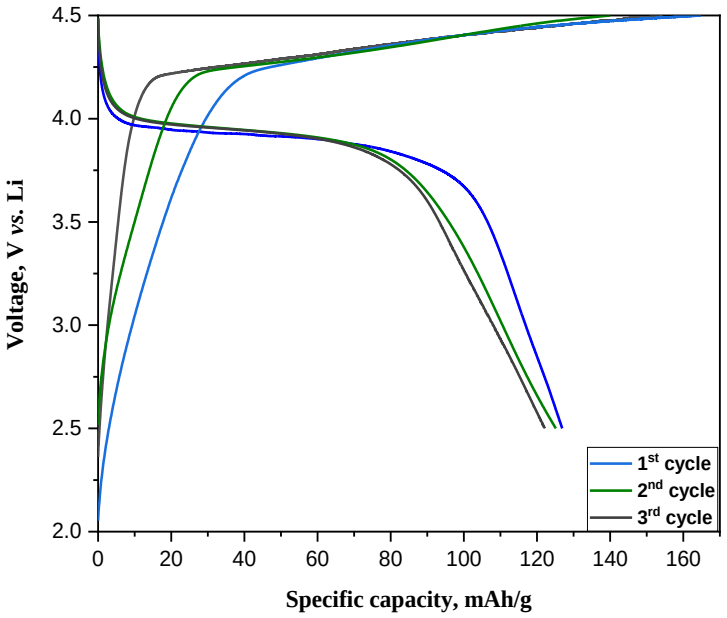

Figure 8. *Charge–discharge profiles of prepared $LiMnPO_4$@C material at 0.05 C-rate*

Conclusions

During this study, the intermediate compound Li_3PO_4 was firstly synthesized by a simple precipitation method. Thereafter, the main material $LiMnPO_4$ was prepared by solvothermal reaction under controlled conditions. The objective of this research was the optimization of solvothermal synthesis parameters using response surface methodology based on Box-Behnken design. Three independent variables were considered in this study, which are the concentration of solvent (PEG), reaction time and reaction temperature. The RSM optimization of operating conditions for the preparation of the pure $LiMnPO_4$ phase was applied. Analysis of variance (ANOVA) confirmed that the proposed regression model is in good agreement with the experimental data, providing a high determination and adjusted determination coefficients.The obtained results confirmed that the optimum conditions for maximum $LiMnPO_4$ phase purity are: c_{PEG} = 0.1 mol l^{-1}, T = 250 °C and τ = 180 min. The material synthesized under optimum conditions was subjected to supplementary characterization techniques to study the crystalline structure and the surface morphology. The results suggested that the used precursors, as well as the synthesis parameters, can directly affect the material purity and the structural properties.

This as-prepared cathode material $LiMnPO_4$@C, can display an initial charge-discharge capacity of 164.8 and 128.8 mAh g^{-1} at 0.05 C-rate, respectively, with moderated initial coulombic efficiency of about 78.2 %. Further investigations on the prepared material (such as particle size reduction, improved carbon coating, *etc.*) will be conducted to improve its electrochemical performance.

References

[1] K. Saravanan, P. Balaya, M. V. Reddy, B. V. R. Chowdari, J. J. Vittal, *Energy and Environmental Science* **3(4)** (2010) 457-464. https://doi.org/10.1039/b923576k

[2] J. Fan, J. Chen, Y. Chen, H. Huang, Z. Wei, M. Zheng, Q. Dong, *Journal of Materials Chemistry A* **2(14)** (2014) 4870-4873. https://doi.org/10.1039/C3TA15210C

[3] B. Kang, G. Ceder, *Nature* **458(7235)** (2009) 190-193. https://doi.org/10.1038/nature07853

[4] S. Ma, M. Jiang, P. Tao, C. Song, J. Wu, J. Wang, T. Deng, W. Shang, *Progress in Natural Science: Materials International* **28(6)** (2018) 653-666. https://doi.org/10.1016/j.pnsc.2018.11.002

[5] J. Zhang, S. Luo, L. Chang, S. Bao, J. Liu, *Electrochimica Acta* **193** (2016) 16-23. https://doi.org/10.1016/j.electacta.2016.02.018

[6] A. K. Padhi, K. S. Nanjundaswamy, J. B. Goodenough, *Journal of the Electrochemical Society* **144(4)** (1997) 1188-1194. https://doi.org/10.1149/1.1837571

[7] M. K. Devaraju, I. Honma, *Advanced Energy Materials* **2(3)** (2012) 284-297. https://doi.org/10.1002/aenm.201100642

[8] J. Wolfenstine, J. Allen, *Journal of Power Sources* **142(1–2)** (2005) 389–90. https://doi.org/10.1016/j.jpowsour.2004.11.024

[9] J. Yang, J. J. Xu, *Journal of the Electrochemical Society* **153(4)** (2006) A716. https://doi.org/10.1149/1.2168410

[10] K. Amine, H. Yasuda, M. Yamachi, *Electrochemical and Solid-State Letters* **3(4)** (2000) 178-179. https://doi.org/10.1149/1.1390994

[11] M. S. Kim, J. P. Jegal, K. C. Roh, K. B. Kim, *Journal of Materials Chemistry A* **2(27)** (2014) 10607-10613. https://doi.org/10.1039/C4TA01197J

[12] C. Delacourt, L. Laffont, R. Bouchet, C. Wurm, J. B. Leriche, M. Morcrette, J. M. Tarascon, C. Masquelier, *Journal of the Electrochemical Society* **152(5)** (2005) 913-921. https://doi.org/10.1149/1.1884787

[13] P. Nie, L. Shen, F. Zhang, L. Chen, H. Deng, X. Zhang, *CrystEngComm.* **14(13)** (2012) 4284-4288. https://doi.org/10.1039/C2CE25094B
[14] Z. X. Nie, C. Y. Ouyang, J. Z. Chen, Z. Y. Zhong, Y. L. Du, D. S. Liu, S. Q. Shi, M.S . Lei, *Solid State Communications* **150(1–2)** (2010) 40-44. https://doi.org/10.1016/j.ssc.2009.10.010
[15] S. Zhong, Y. Xu, Y. Li, H. Zeng, W. Li, J. Wang, *Rare Metals* **31(5)** (2012) 474-478. https://doi.org/10.1007/s12598-012-0542-3
[16] H. C. Dinh, S. Il Mho, Y. Kang, I. H. Yeo, *Journal of Power Sources* **244** (2013) 189-195. https://doi.org/10.1016/j.jpowsour.2013.01.191
[17] M. Pivko, M. Bele, E. Tchernychova, N. Z. Logar, R. Dominko, M. Gaberscek, *Chemistry of Materials* **24(6)** (2012) 1041-1047.https://doi.org/10.1021/cm203095d
[18] J. Yoshida, M. Stark, J. Holzbock, N. Hüsing, S. Nakanishi, H. Iba, H. Abe, M. Naito, *Journal of Power Sources* **226** (2013) 122-126. https://doi.org/10.1016/j.jpowsour.2012.09.081
[19] P. Barpanda, K. Djellab, N. Recham, M. Armand, J. M. Tarascon, *Journal of Materials Chemistry* **21(27)** (2011) 10143-10152. https://doi.org/10.1039/C0JM04423G
[20] Z. Bakenov, I. Taniguchi, *Journal of Power Sources* **195(21)** (2010) 7445-7451. https://doi.org/10.1016/j.jpowsour.2010.05.023
[21] T. N.L. Doan, Z. Bakenov, I. Taniguchi, *Advanced Powder Technology* **21(2)** (2010) 187-196. https://doi.org/10.1016/j.apt.2009.10.016
[22] T. N. L. Doan, I. Taniguchi, *Journal of Power Sources* **196(3)** (2011) 1399-1408. https://doi.org/10.1016/j.jpowsour.2010.08.067
[23] L. Damen, F. De Giorgio, S. Monaco, F. Veronesi, M. Mastragostino, *Journal of Power Sources* **218** (2012) 250-253. https://doi.org/10.1016/j.jpowsour.2012.06.090
[24] R. El Khalfaouy, S. Turan, K. B. Dermenci, U. Savaci, A. Addaou, A. Laajeb, A. Lahsini, *Ceramics International* **45(14)** (2019) 17688-17695. https://doi.org/10.1016/j.ceramint.2019.05.336.
[25] R. El Khalfaouy, A. Addaou, A. Laajeb, A. Lahsini, *Journal of Alloys and Compounds* **775** (2019) 836-844. https://doi.org/10.1016/j.jallcom.2018.10.161
[26] R. El-Khalfaouy, S. Turan, M. A. Rodriguez, K. B. Dermenci, U. Savacı, A. Addaou, A. Laajeb, A. Lahsini, *Journal of Applied Electrochemistry* **51(4)** (2021) 681-689. https://doi.org/10.1007/s10800-020-01528-8
[27] Z. Bakenov, I. Taniguchi, *Electrochemistry Communications* **12(1)** (2010) 75-78. https://doi.org/10.1016/j.elecom.2009.10.039
[28] N.-H. Kwon, T. Drezen, I. Exnar, I. Teerlinck, M. Isono, M. Graetzel, *Electrochemical and Solid-State Letters* **9(6)** (2006) A277. https://doi.org/10.1149/1.2191432
[29] D. Di, T. Hu, J. Hassoun, *Journal of Alloys and Compounds* **693** (2017) 730-737. https://doi.org/10.1016/j.jallcom.2016.09.193
[30] S. Luo, Y. Sun, S. Bao, J. Li, J. Zhang, T. Yi, *Journal of Electroanalytical Chemistry* **832** (2019) 196-203. https://doi.org/10.1016/j.jelechem.2018.10.062
[31] S.F. Yang, P.Y. Zavalij, M.S. Whittingham, *Electrochemistry Communications* **3(9)** (2001) 505-508. https://doi.org/10.1016/S1388-2481(01)00200-4
[32] G. Chen, J. D. Wilcox, T. J. Richardson, *Electrochemical and Solid-State Letters* **11(11)** (2008) A190. https://doi.org/10.1149/1.2971169
[33] K. Zhu, W. Zhang, J. Du, X. Liu, J. Tian, H. Ma, S. Liu, Z. Shan, *Journal of Power Sources* **300** (2015) 139-146. https://doi.org/10.1016/j.jpowsour.2015.08.065
[34] R. El Khalfaouy, A. Elabed, A. Addaou, A. Laajeb, A. Lahsini, *Arabian Journal for Science and Engineering* **44** (2019) 123-129. https://doi.org/10.1007/s13369-018-3248-5
[35] Y. Cao, J. Duan, G. Hu, F. Jiang, Z. Peng, *Electrochimica Acta* **98** (2013) 183-189. https://doi.org/10.1016/j.electacta.2013.03.014

[36] R. El Khalfaouy, A. Addaou, A. Laajeb, A. Lahsini, *International Journal of Hydrogen Energy* **44(33)** (2019) 18272-18282. https://doi.org/10.1016/j.ijhydene.2019.05.129
[37] S. Vedala, M. Sushama, *Materials Today: Proceedings* **5(1)** (2018) 1649-1656. https://doi.org/10.1016/j.matpr.2017.11.259
[38] T. Drezen, N. H. Kwon, P. Bowen, I. Teerlinck, M. Isono, I. Exnar, *Journal of Power Sources* **174(2)** (2007) 949-953. https://doi.org/10.1016/j.jpowsour.2007.06.203
[39] N. N. Bramnik, H. Ehrenberg, *Journal of Alloys and Compounds* **464(1–2)** (2008) 259-264. https://doi.org/10.1016/j.jallcom.2007.09.118
[40] J. Su, B.Q. Wei, J.P. Rong, W. Y. Yin, Z. X. Ye, X. Q. Tian, L. Ren, M. H. Cao, C. W. Hu, *Journal of Solid State Chemistry* **184(11)** (2011) 2909-2919. https://doi.org/10.1016/j.jssc.2011.08.042
[41] S. L. Yang, R. G. Ma, M. J. Hu, L. J. Xi, Z. G. Lu, C. Y. Chung, *Journal of Materials Chemistry* **22(48)** (2012) 25402-25408. https://doi.org/10.1039/C2JM34193J
[42] W. Zhang, Z. Shan, K. Zhu, S. Liu, X. Liu, J. Tian, *Electrochimica Acta* **153** (2015) 385-392. https://doi.org/10.1016/j.electacta.2014.12.012
[43] C. M. Borror, *Journal of Quality Technology* **39(3)** (2007) 297. https://doi.org/10.1080/00224065.2007.11917695
[44] M. Mir, S. M. Ghoreishi, *Chemical Engineering and Technology* **38(5)** (2015) 835-843. https://doi.org/10.1002/ceat.201300328
[45] L. Cesar, S. Garcia-Segura, N. Bocchi, E. Brillas, *Applied Catalysis B* **103(1–2)** (2011) 21-30. https://doi.org/10.1016/j.apcatb.2011.01.003
[46] J. Herney-Ramirez, M. Lampinen, M. A. Vicente, C. A. Costa, L. M. Madeira, *Industrial and Engineering Chemistry Research* **47(2)**(2008) 284-294.https://doi.org/10.1021/ie070990y
[47] A. Long, H. Zhang, Y. Lei, *Separation and Purification Technology* **118** (2013) 612-619. https://doi.org/10.1016/j.seppur.2013.08.001
[48] T. Xu, Y. Liu, F. Ge, L. Liu, Y. Ouyang, *Applied Surface Science* **280** (2013) 926-932. https://doi.org/10.1016/j.apsusc.2013.05.098
[49] H. Xu, S. Qi, Y. Li, Y. Zhao, J. W. Li, *Environmental Science and Pollution Research* **20** (2013) 5764-5772. https://doi.org/10.1007/s11356-013-1578-0
[50] J. Wu, H. Zhang, N. Oturan, Y. Wang, L. Chen, M. A. Oturan, *Chemosphere* **87(6)** (2012) 614-620. https://doi.org/10.1016/j.chemosphere.2012.01.036
[51] R. Muruganantham, M. Sivakumar, R. Subadevi, *Journal of Power Sources* **300** (2015) 496-506. https://doi.org/10.1016/j.jpowsour.2015.09.103
[52] Y. Hong, Z. Tang, S. Wang, W. Quan, Z. Zhang, *Journal of Materials Chemistry A* **3(19)** (2015) 10267-10274. https://doi.org/10.1039/C5TA01218J
[53] S.-Y. Cao,L.-J. Chang,S.-H. Luo ,X.-L. Bi, A.-L. Wei, J.-N. Liu, *Particle and Particle Systems Characterization* **39(2)** (2021) 2100203. https://doi.org/10.1002/ppsc.202100203
[54] D. Fujimoto, Y. Lei, Z.-H. Huang, F. Kang, J. Kawamura, *International Journal of Electrochemistry* **2014** (2014) 768912. https://doi.org/10.1155/2014/768912
[55] D. Choi, D. Wang, I. T. Bae, J. Xiao, Z. Nie, W. Wang, V. V. Viswanathan, Y. J. Lee, J. G. Zhang, G. L. Graff, Z. Yang, J. Liu, *Nano Letters* **10(8)** (2010) 2799-2805. https://doi.org/10.1021/-nl1007085